Journal of Applied Polymer Science

Inkjet printing of polylactic acid on substrates prepared by fused deposition modeling and its potential for selective surface finishing

Thomas Köpplmayr, Michael Mühlberger
Profactor GmbH, Im Stadtgut A2, Steyr-Gleink 4407, Austria
Correspondence to: T. Köpplmayr (E-mail: thomas.koepplmayr@profactor.at)

ABSTRACT: Fused deposition modeling (FDM) is an additive manufacturing technology commonly used for prototyping. One limiting aspect for the use in functional prototyping and small-lot production is the achievable surface roughness. The aim of this work was to investigate a potential method of processing polylactic acid (PLA), as it is commonly used for FDM printing, via inkjet technology. PLA solvent inks with different concentrations were prepared by dissolving PLA in 1,4-dioxane. The tested PLA substrates were prepared by FDM with different layer thicknesses and the change in surface roughness after multilayer inkjet printing was measured by a stylus profilometer. The surface roughness was reduced by up to 50% and further increasing the number of inkjet layers caused voids and PLA accumulations. © 2016 Wiley Periodicals, Inc. J. Appl. Polym. Sci. **2016**, *133*, 43527.

KEYWORDS: coatings; manufacturing; rheology; surfaces and interfaces; thermoplastics

Received 11 December 2015; accepted 9 February 2016
DOI: 10.1002/app.43527

INTRODUCTION

Fused deposition modeling (FDM) is a mold-less manufacturing method that involves layer-wise deposition of thermoplastic materials. Although this technology is commonly used for modeling, prototyping, and small-lot production applications, the achievable surface roughness is one of its most limiting aspects.[1–3] Layer thickness and part orientation proved to be the significant factors in determining the surface quality of a printed part.[4] Due to the layer-by-layer generation of the printed part a staircase effect appears, which cannot be eliminated by the printer itself. In general, a thinner slice layer produces better surface finish but it will increase the build time. Anitha *et al.*[5] discovered that layer thickness is the most influencing process parameter affecting surface roughness followed by road width and deposition speed. Thrimurthulu *et al.*[6] presented an approach that determines the optimal part deposition orientation using adaptive slicing. Lan *et al.*[7] used a similar technique for stereolithography parts. As rapid prototyping is moving towards rapid manufacturing there is an increasing demand for good quality parts. Surface finishing is critical not only for better functionality and look, but also for cost reduction in terms of reduced post-processing of parts.[8]

Basically, two primary approaches are used to achieve smooth surfaces on parts: chemical and mechanical smoothing. Chemical smoothing systems expose the part to solvent vapors, which are allowed to condense on the surface and partially dissolve it to smooth small ridges. Mechanical abrasion may also be used to smooth part surfaces, although this has limitations on parts with complex surface geometries due to inherent difficulties in abrasive materials entering small features.[9] Pandey *et al.* developed a simple material removal method named hot cutter machining (HCM), which is able to produce surface finish of the order of 0.3 mm with 87% confidence level.[10] Based on their findings, they proposed a virtual hybrid FDM system that uses both layer-by-layer deposition and machining.[11]

In addition to modifying the fabricated part itself, the application of surface coatings is another approach for surface finishing. It does not only reduce the surface roughness, but also improves the mechanical strength, especially if wear-resistant surfaces are needed.[12] Moreover, sealing may be necessary for fluid pressure applications due to porosities, air gaps, and voids in FDM parts. Through brushing, excess sealant can accumulate at certain features that can significantly alter part dimensions. To reduce dimensional changes and to enable the sealant to infiltrate the FDM part, vacuum infiltration is used wherein the porous part is exposed to a fluid in vacuum allowing the fluid to fill the pores within the part.[13]

Inkjet printing is an attractive patterning technology, which has become increasingly accepted for a variety of industrial and scientific applications. Apart from conventional document printing, the inkjet technology has been successfully applied in the areas of electronics, mechanical engineering, and life sciences.[14] An inkjet printer is a dosing robot, which deposits ink materials only in a desired location and allows for selective surface

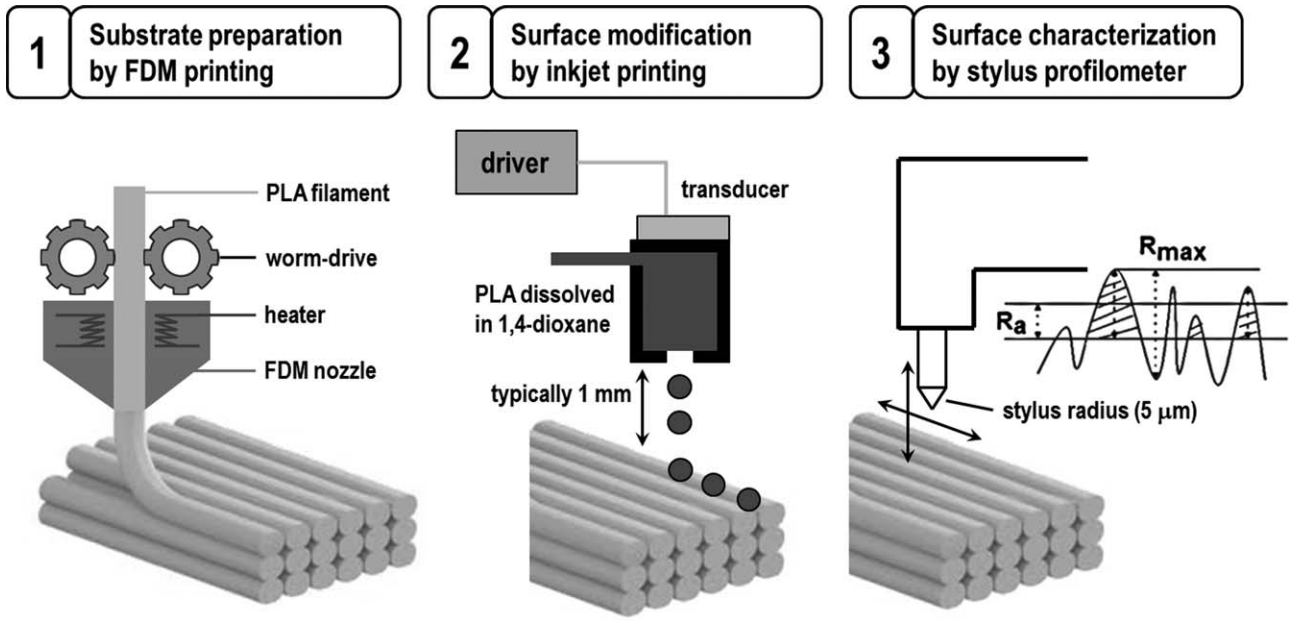

Figure 1. Experimental steps including substrate preparation by FDM printing, surface modification by inkjet printing, and surface characterization by mechanical profilometry.

modification. Polymer melts are too viscous to print via inkjet and therefore, either a dilute solution is used or reactive components are printed and cured in a post-processing step. For polylactic acid (PLA) grades which are processed via FDM, 1,4-dioxane proved to be a good solvent and simple surface finishing by dipping or polishing has been explored by the Reprap community.[15] Also, 1,4-dioxane is often used as solvent when creating PLA phase-separated scaffolds.[16] Its physical properties are very convenient for inkjet printing due to its high boiling point of 101 °C and its compatibility with the used cartridge and printhead. In our study, we prepared PLA solvent inks with different concentrations by dissolving PLA in 1,4-dioxane and investigated the printability using a drop-on-demand (DOD) inkjet printer. On the application of voltage pulses, ink drops are ejected by a pressure wave created by mechanical motions of a piezoelectric actuator. The experimental steps are summarized in Figure 1. Our experiments show promising results in selectively depositing small amounts of material in well-defined areas on the printed parts.

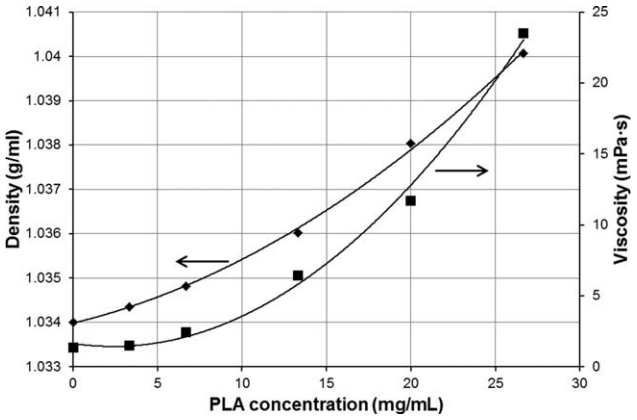

Figure 2. Fluid density (◆) and dynamic viscosity (■) for different PLA concentrations.

EXPERIMENTAL

Digital designs were created using the 3D CAD program Solidworks (Dassault Systèmes, Waltham, Massachusetts) and printed using a Makerbot Replicator (MakerBot Industries, LLC, New York City). The MakerWare software uses proprietary strategies for the conversion of the design to a 3D printable format. This is achieved by slicing the design into layers and determining the tool path for the printer to lay down the printing materials. Flat substrates were printed out of PLA (filament with 1.75 mm in diameter) using 0.15 mm, 0.2 mm or 0.3 mm layer thickness and a nozzle temperature of 220 °C. The nozzle diameter was 0.4 mm and 10% infill with two shell layers were used.

The surface topography of the samples was pictured using a Bruker Veeco Dektak 150 Stylus profilometer (Bruker Corporation, Billerica, Massachusetts). The arithmetic and quadratic means of the measured amplitude values based on the vertical deviations of the roughness profile from the mean line were used as values to characterize the surface roughness (R_a and R_q values). Images were taken over a total area of 4 × 4 mm^2 with 100 measured lines per sample (stylus radius 5 μm).

Slices of the PLA filament were dissolved in 1,4-dioxane (purchased from Sigma-Aldrich) at different polymer concentrations. The polymer solution was stirred for 2 h at 65 °C and then was passed through a syringe filter (pore size 5 μm) to eliminate insoluble particles. The viscosity was measured with a vibrational viscometer (SV-10 Viscometer, A&D Company Ltd., Tokyo, Japan). The surface tension was measured with a dynamic contact angle analyzer (DSA100, Krüss GmbH, Hamburg, Germany) and the fluid density was measured with a

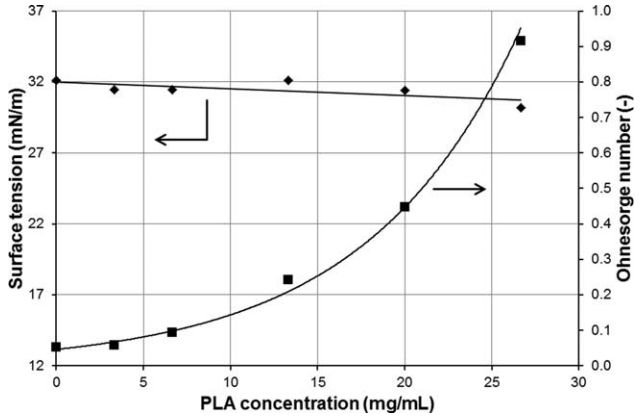

Figure 3. Surface tension (◆) and resulting Ohnesorge numbers (■) for different PLA concentrations (nozzle diameter $d = 21$ μm).

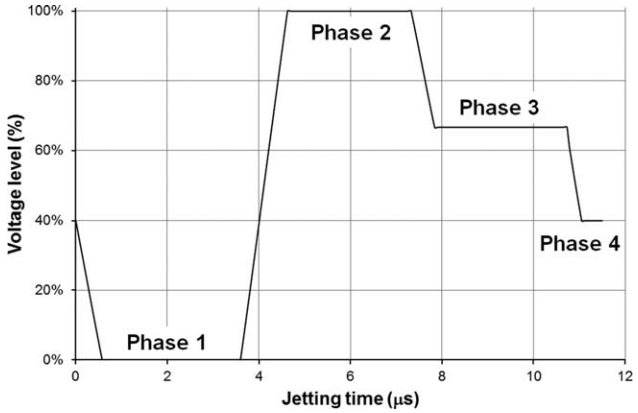

Figure 5. Conventional waveform for inkjet printing consisting of four phases.

specific gravity bottle according to Gay-Lussac (Paul Marienfeld GmbH & Co. KG, Lauda Königshofen, Germany).

Inkjet printing was conducted on a piezoelectric DOD inkjet printer (Dimatrix Materials Printer, DMP-2800). A waveform editor and a drop-watch camera system allows manipulation of the electronic pulses to the piezo jetting device for optimization of the drop characteristics as it is ejected from the nozzle. The inkjet printability of PLA inks was investigated under different processing conditions. The head temperature of the cartridge was set to 30 °C and the firing voltage varied over a range of 24–38 V. FDM parts or PLA foils provided by Pütz GmbH + Co. Folien KG were used as substrates.

Surface wetting was investigated using contact angle measurements (sessile drop method) which can be related to surface tensions or energies via Young's equation[17]

$$\sigma_s = \gamma_{sl} + \sigma_l \cos\theta \tag{1}$$

where θ is the measured contact angle, γ_{sl} is the surface tension of the solid–liquid interface and σ is the surface tension of the solid–vapor (s) or liquid–vapor (l) interface. Following Owens–Wendt–Kaelble,[18–20] an expression for γ_{sl} can be combined with eq. (1) and results in a relation between the contact angle and the liquid's surface tension from which the solid's surface energy can be extracted.

$$\gamma_{sl} = \sigma_s + \sigma_l - 2 \cdot \left(\sqrt{\sigma_s{}^d \cdot \sigma_l{}^d} + \sqrt{\sigma_s{}^p \cdot \sigma_l{}^p} \right) \tag{2}$$

The dispersive (d) and polar (p) solid surface energy components of the PLA foil were calculated by measuring the contact angles of three different liquids (water, diiodomethane, and ethylene glycol) whose polar and dispersive components were known on the solid surface. Consequently, solid surface energy components can be extracted from a linear fit to eq. (3), derived from the Owens–Wendt–Kaelble and Young's equations:

$$\frac{\sigma_l \cdot (\cos\theta + 1)}{2\sqrt{\sigma_l{}^d}} = \frac{\sqrt{\sigma_l{}^p \cdot \sigma_s{}^p}}{\sqrt{\sigma_l{}^d}} + \sqrt{\sigma_s{}^d} \tag{3}$$

The total surface tension σ_l of the developed ink was measured by the pendant drop method, which involves the determination of the profile of a drop of a liquid at mechanical equilibrium.

Besides inkjet printing, treatment with 1,4-dioxane vapor was used to smoothen the FDM part. A rag was dipped into the solvent and put into a beaker glass together with the sample. The glass was put upside down into an oven at 50 °C and the sample was exposed to the vapor for 30 min.

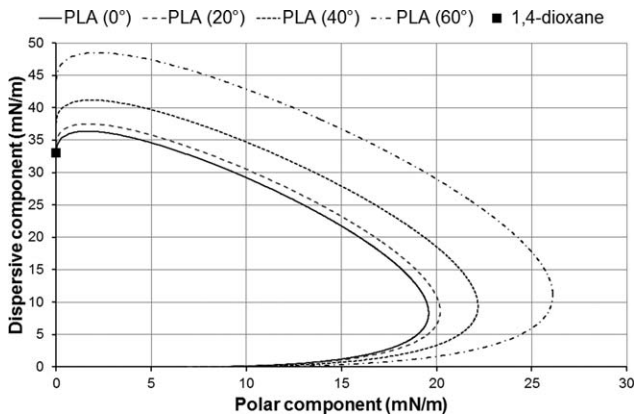

Figure 4. Wetting envelope of a PLA foil with different contact angles. For inks based on 1,4-dioxane ($\sigma_l{}^d$, $\sigma_l{}^p$ from Cappelletti *et al.*[22]), complete wetting can be expected.

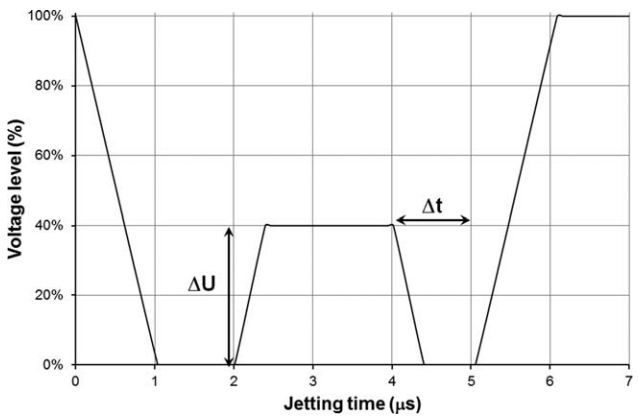

Figure 6. A double waveform for control of droplet formation for low viscosity fluids (ΔU, height of first pulse; Δ*t*, duration between first and second pulse).

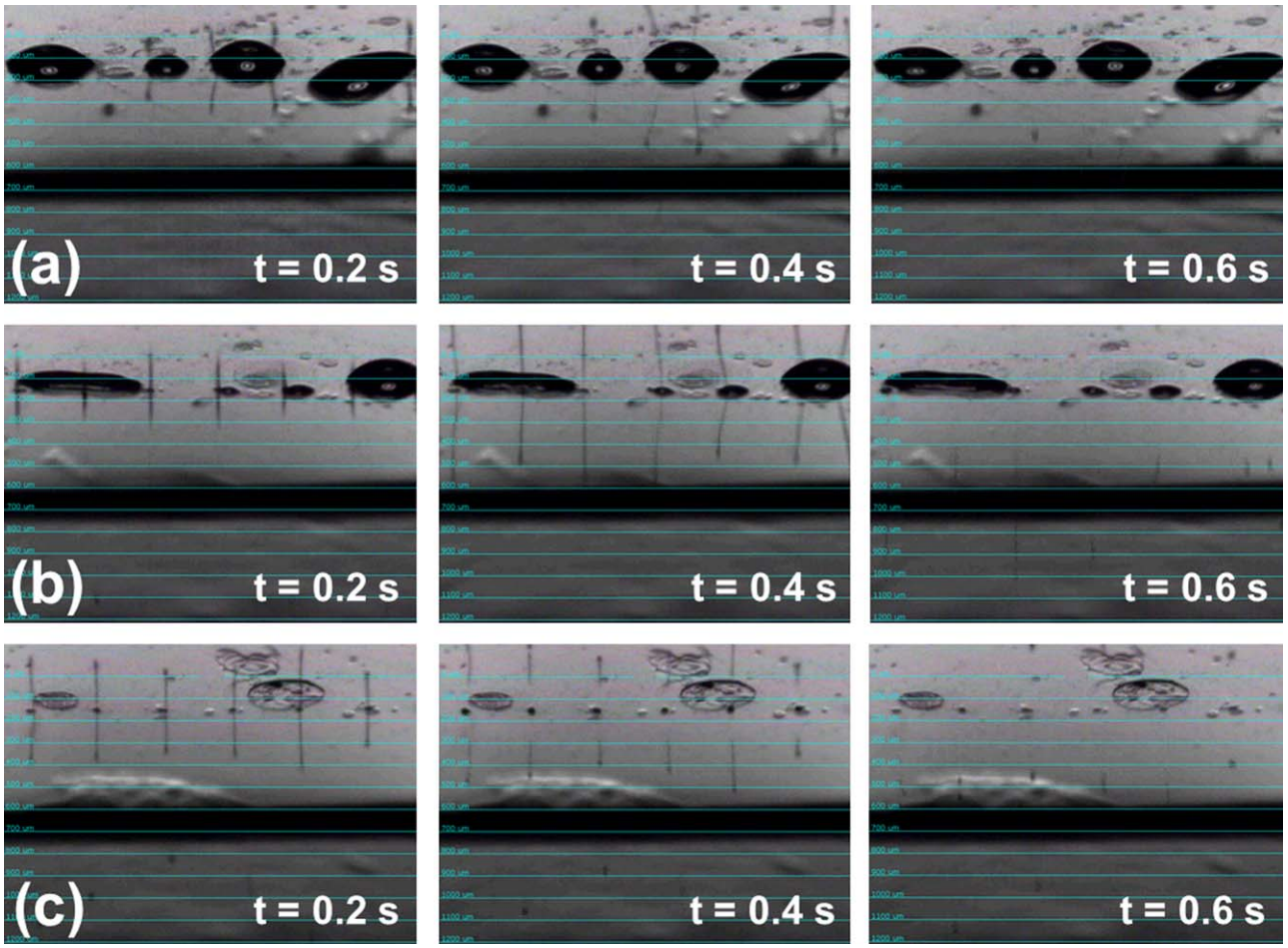

Figure 7. Drop formation of 3 mg/mL PLA in 1,4-dioxane ($\eta = 1.5$ mPa s) with changing waveform parameters: (a) $\Delta U = 100\%$ and $\Delta t = 3$ ms, (b) $\Delta U = 40\%$ and $\Delta t = 6$ ms, and (c) $\Delta U = 40\%$ and $\Delta t = 1$ ms. The droplet ejecting direction is from top to bottom and large droplets are formed by ink accumulation during printing with (a) and (b). [Color figure can be viewed in the online issue, which is available at wileyonlinelibrary.com.]

RESULTS AND DISCUSSION

The behavior of fluids during inkjet printing can be represented by the Reynolds, Weber, and Ohnesorge numbers[21]

$$\mathrm{Re} = \frac{v\rho d}{\eta}, \quad \mathrm{We} = \frac{v^2 \rho d}{\sigma_l}, \quad \mathrm{Oh} = \frac{\sqrt{\mathrm{We}}}{\mathrm{Re}} = \frac{\eta}{\sqrt{\sigma_l \rho d}} \tag{4}$$

where ρ, η, and σ_l are the density, dynamic viscosity, and surface tension of the fluid respectively; v is the velocity; and d is the nozzle diameter. The Ohnesorge number (Oh) includes all physical constants to characterize drop generation in an inkjet printer and is used as a printing indicator. It relates the viscous forces to inertial forces and surface tension. Thus, it describes the tendency of stable drop formation. The number was defined by Wolfgang von Ohnesorge, 1936, in his doctoral thesis.[21] If $\mathrm{Oh} > 1$, viscous dissipation prevents drop ejection from the printer and if $\mathrm{Oh} < 0.1$, droplets are accompanied by unwanted satellite drops. Increasing the PLA concentration in the ink mainly influences the dynamic viscosity (Figure 2) which results in higher Ohnesorge numbers, while the surface tension remains almost constant (Figure 3). For PLA concentrations above 7 mg/mL the Ohnesorge number is within the required printing regime.

The profile of a drop of ink was determined by the balance between gravity and surface forces. To predict how well a PLA surface is wetted by the ink, we compared the ink's surface tension with the surface free energy of the PLA substrate using the polar and dispersive contributions to the total energy. The method yields the so-called wetting envelope in polar coordinates with radius r and angle φ as given in the following equation:

$$r = 2 \cdot \frac{\left(\sqrt{\cos\phi \cdot {\sigma_s}^d} + \sqrt{\sin\phi \cdot {\sigma_s}^p}\right)^2}{(\cos\phi + \sin\phi)^2}, \quad {\sigma_l}^p = r \cdot \sin\phi, \quad {\sigma_l}^d = r \cdot \cos\phi \tag{5}$$

A prediction of an ink's wetting behavior is obtained by comparing the surface tension of the ink with the wetting envelope of the surface. Complete wetting is obtained for an ink with dispersive and polar coordinates within the area confined by the

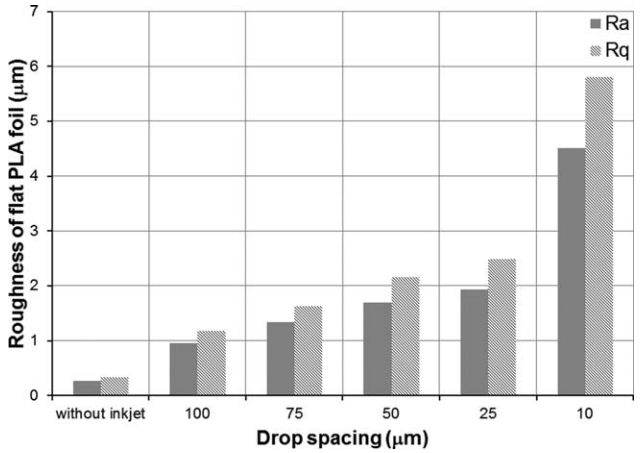

Figure 8. Change of surface roughness of a flat PLA foil after single-layer inkjet printing of 3 mg/mL PLA in 1,4-dioxane ($\eta = 1.5$ mPa s) by varying the drop spacing.

x- and y-axis and the curve for $\theta = 0°$ and partial wetting occurs for inks with polar and dispersive coordinates lying outside of the envelope. At large contact angles ($> 90°$) the ink will dewet the surface while drying and the resulting film will not be homogeneous. The used solvent 1,4-dioxane shows dispersive and polar coordinates[22] within the wetting envelope of an uncoated PLA foil (Figure 4). Thus, for our inks complete wetting can be expected.

The print quality delivered by an inkjet printhead depends on the properties of the jetted drop, i.e. the drop velocity, the jetting direction, and the drop volume. The relationship between velocity and volume can be altered for different actuation waveforms. During printing of our inks using a standard waveform, drop formation failed for each PLA dilution. Due to fast evaporation, PLA precipitated on the nozzle plate and blocked the nozzle. Printing of the pure solvent (1,4-dioxane) also failed due to splashing. For the observation of active print nozzles, a dropwatcher was used to investigate droplet and printhead characteristics. The aim at this stage was to optimize the printing parameters for droplet formation and to achieve single regular ink droplet formation.

A conventional waveform usually consists of four phases as shown in Figure 5. At the beginning, the piezo element is slightly deflected prior to the initiation of the drive pulse train. In the first phase, a decrease to zero volts brings the piezo back to a relaxed position. Then, the chamber is compressed and

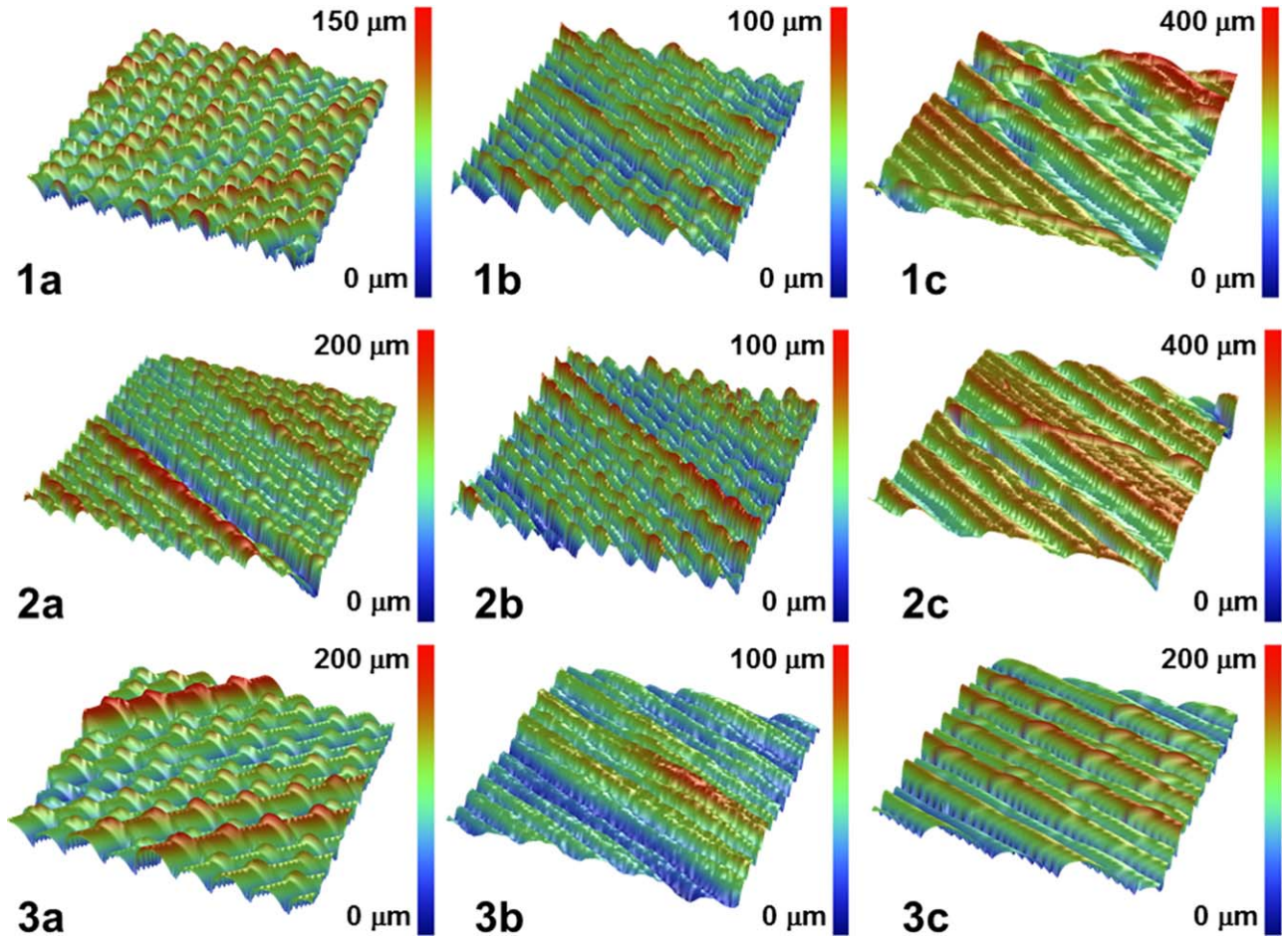

Figure 9. Multilayer inkjet printing of 3 mg/mL PLA in 1,4-dioxane ($\eta = 1.5$ mPa s, 10 μm drop spacing) on substrates prepared by FDM, (1–3a) original surface with 0.15 mm, 0.2 mm or 0.3 mm layer thickness, (1–3b) 10 layers inkjet, (1–3c) 20 layers inkjet. [Color figure can be viewed in the online issue, which is available at wileyonlinelibrary.com.]

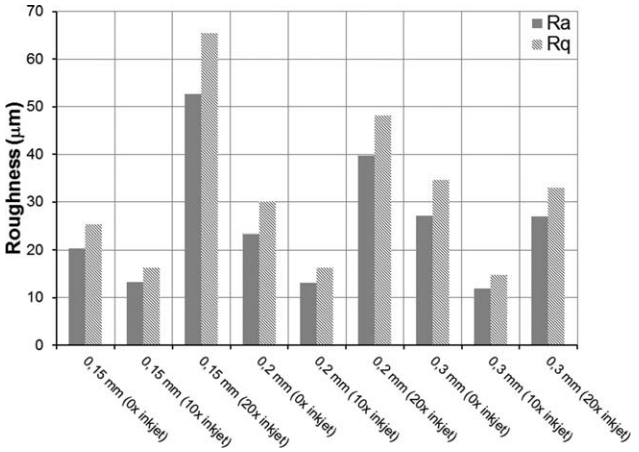

Figure 10. Change of surface roughness of a FDM part printed with various layer thicknesses after multilayer inkjet printing of 3 mg/mL PLA in 1,4-dioxane ($\eta = 1.5$ mPa s, 10 μm drop spacing).

pressure is generated to form and eject a drop (phase 2). After jetting, the chamber decompresses at first only partially (phase 3) and then in full (phase 4).

To overcome the lower limit of fluid viscosity, double waveforms with two square pulses (Figure 6) can be applied to control the droplet formation in the piezoelectric inkjet nozzle.[23] With regard to the double waveforms, the effect of driving voltage (ΔU) and time separation (Δt) between the pulses was investigated. Good drop formation was achieved at $\Delta U = 40\%$ (total voltage 24 V) and $\Delta t = 1$ ms for the 3 mg/mL PLA ink, while higher voltage levels or longer time separation caused ink accumulation at the nozzle and satellite droplets (Figure 7). At concentrations of 7 mg/mL or higher, precipitated PLA again blocked the nozzle.

Besides choosing the appropriate combination of solvent and substrate, also the drop spacing is crucial to obtain homogeneous films. In general, printing droplets with large dot spacing leads to individual dots, while decreasing the dot spacing revealed scalloped lines. We investigated five dot spacings (10 µm, 25 µm, 50 µm, 75 µm, and 100 µm) on a flat PLA foil and due to the good wetting, no individual dots were observed. The solvent partially dissolves the PLA substrate and thus increases the surface roughness of the PLA foil as shown in Figure 8. However, at 25 µm dot spacing, still a few isolated unwetted areas can be found and, therefore, 10 µm dot spacing was used for inkjet printing on FDM parts. In addition to the reduction of the drop spacing, multilayer inkjet printing (10 layers) was applied to significantly change the surface roughness as higher amounts of PLA and solvent are necessary to smoothen the surface. Wetting of FDM parts is more challenging due to the typical layer composition, which increases the free surface area and causes capillary forces influencing the wetting behavior. Further increasing the number of inkjet layers to 20, caused voids and PLA accumulations. Our experiments show promising results in selectively depositing small amounts of material in well-defined areas on the printed parts as shown in Figure 9. The surface roughness of the original filament structure changes due to the deposition of PLA from the ink (1,4-dioxane evaporates) as well as swelling and partially dissolving of the PLA substrate by 1,4-dioxane.

During FDM, the used layer thickness also influences the resulting surface roughness of the printed part. We tested layer thicknesses of 0.15 mm, 0.2 mm, and 0.3 mm, which produced R_a values of 20 µm, 23 µm, and 27 µm, respectively. After inkjet printing of 10 layers, the surface roughness could be reduced to about 13 µm independent of the previously used layer thickness (Figure 10). Further increasing the number of inkjet layers to 20, again caused voids and PLA accumulations resulting in higher surface roughness whereas lower initial R_a values are influenced more strongly by the multilayer inkjet process. The achieved surface roughness using 10 layers inkjet printing was comparable to vapor treatment (Figures 11 and 12), but could be applied in a selective manner with less amount of solvent and lower ambient contamination.

Figure 13 shows some photographs of flat PLA parts, which were prepared by FDM and modified using 10 layer inkjet printing. The original surface consists of sharp peaks due to the layer-wise manufacturing process. After inkjet modification, the surface roughness decreases and the printed area receives a more glossy appearance.

CONCLUSIONS

The aim of this work was to investigate a potential method of processing PLA via inkjet technology, which provides the advantage of selectively depositing small amounts of material on certain areas of a FDM part in a more automated manner

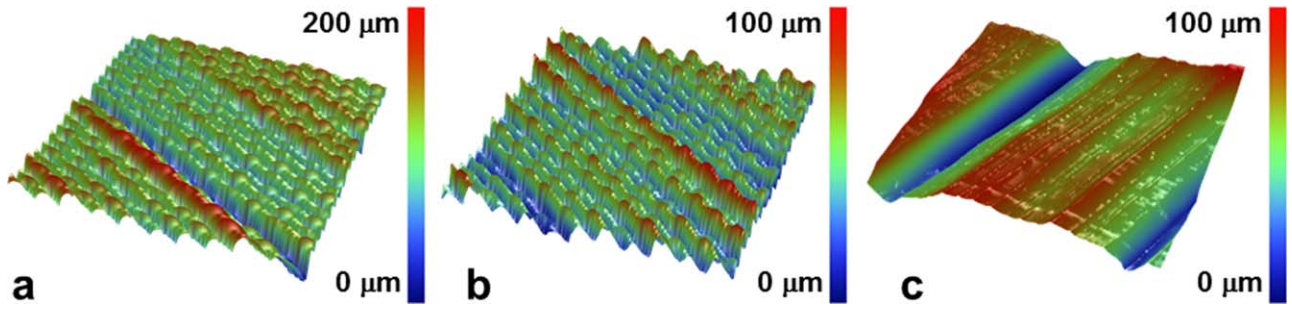

Figure 11. Comparison of surface topography change of a FDM part (a) printed with 0.2 mm layer thicknesses (b) after 10 layers inkjet printing of 3 mg/mL PLA in 1,4-dioxane ($\eta = 1.5$ mPa s, 10 μm drop spacing) or (c) treatment with 1,4-dioxane vapor for 30 min at 50 °C. [Color figure can be viewed in the online issue, which is available at wileyonlinelibrary.com.]

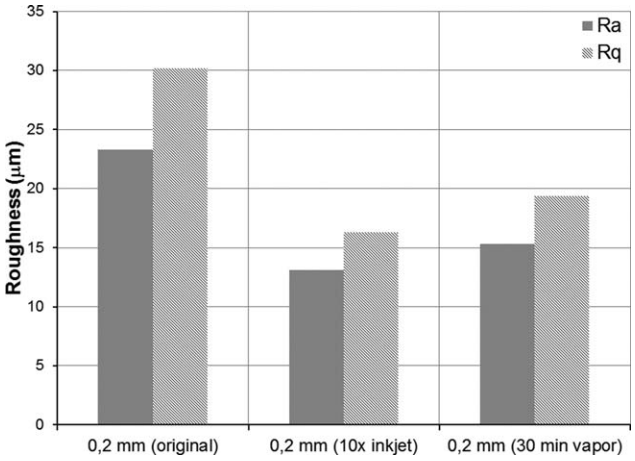

Figure 12. Comparison of surface roughness change of a FDM part printed with 0.2 mm layer thicknesses after 10 layers inkjet printing of 3 mg/mL PLA in 1,4-dioxane ($\eta = 1.5$ mPa s, 10 μm drop spacing) or treatment with 1,4-dioxane vapor for 30 min at 50 °C.

compared to conventional methods like coating, spraying or dipping. PLA solvent inks with different concentrations were prepared by dissolving PLA in 1,4-dioxane. Fluid viscosity and surface tension were crucial parameters in the development of the ink. Ohnesorge numbers were calculated and used as a printing indicator. Contact angle measurements were used to investigate the wetting behavior of the ink on PLA substrates. The influences of waveform peak height, time gap, printing voltage, and dot spacing on droplet formation were also optimized. To overcome the lower limit of fluid viscosity, double waveforms with two square pulses were applied to control droplet formation in the piezoelectric inkjet nozzle. The tested PLA substrates were prepared by FDM with different layer thicknesses and the change in surface roughness after multilayer inkjet printing was measured by a stylus profilometer. After inkjet printing of 10 layers, the surface roughness could be reduced to about 13 μm (up to 50%) independent of the previously used layer thickness in FDM fabrication, which is accompanied by a more glossy appearance of the modified surface. The achieved

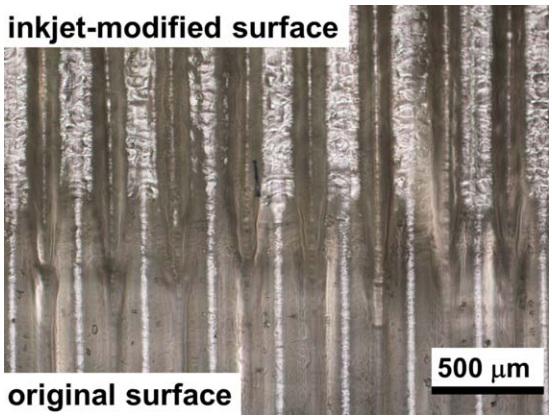

Figure 13. Micrograph of a flat PLA part prepared by FDM and post-processing using 10 layer inkjet printing of 3 mg/mL PLA in 1,4-dioxane ($\eta = 1.5$ mPa s, 10 μm drop spacing). [Color figure can be viewed in the online issue, which is available at wileyonlinelibrary.com.]

surface roughness was comparable to vapor treatment, but could be applied in a selective manner with less amount of solvent and lower ambient contamination. In order to be able to deposit higher amounts of ink, DOD printheads with larger nozzle diameters might be used. Moreover, the continuous inkjet (CIJ) method could be used instead, where a high-pressure pump directs liquid ink from a reservoir through a nozzle, creating a continuous stream of ink droplets, which are then charged in an electrostatic field and finally directed by electrostatic deflection plates to print on the substrate. Nozzle clogging is less likely as the jet is always in use. However, in CIJ, the ink system requires active solvent regulation to counter solvent evaporation during the time of flight, viscosity has to be monitored, and the solvent must be added to counteract solvent loss during printing.

ACKNOWLEDGMENTS

This work was carried out within the research project "Additive Nanoimprinting and Inkjet Printing on Freeform Surfaces (ANIIPF)". Financial support by the Austrian Ministry for Transport, Innovation and Technology (bmvit) is gratefully acknowledged. The authors thank Pütz GmbH + Co. Folien KG for providing the PLA foils for inkjet experiments.

REFERENCES

1. Bual, G. S.; Kumar, P. *Manuf. Sci. Technol.* **2014**, *2*, 51.
2. Mahesh, M.; Wong, Y. S.; Fuh, J. Y. H.; Loh, H. T. *Rapid Prototyping J.* **2004**, *10*, 123.
3. Ahn, D.; Kweon, J. H.; Kwon, S.; Song, J.; Lee, S. *J. Mater. Process. Technol.* **2009**, *209*, 5593.
4. Vasudevarao, B.; Natarajan, D. P.; Henderson, M.; Razdan, A. In Solid Freeform Fabrication (SFF) Symposium; University of Texas: Austin, **2000**; p 251.
5. Anitha, R.; Arunachalam, S.; Radhakrishnan, P. *J. Mater. Process. Technol.* **2001**, *118*, 385.
6. Thrimurthulu, K.; Pandey, P. M.; Reddy, N. V. *Int. J. Mach. Tool Manuf.* **2004**, *44*, 585.
7. Lan, P. T.; Chou, S. Y.; Chen, L. L.; Gemmill, D. *Comput. Aided Des.* **1997**, *29*, 53.
8. Alexander, P.; Allen, S.; Dutta, D. *Comput. Aided Des.* **1998**, *30*, 343.
9. Turner, B. N.; Strong, R.; Gold, S. A. *Rapid Prototyping J.* **2014**, *20*, 192.
10. Pandey, P. M.; Reddy, N. V.; Dhande, S. G. *J. Mater. Process. Technol.* **2003**, *132*, 323.
11. Pandey, P. M.; Reddy, N. V.; Dhande, S. G. *Virtual Phys. Prototyp.* **2006**, *1*, 101.
12. Lee, C. W.; Chua, C. K.; Cheah, C. M.; Tan, L. H.; Feng, C. *Int. J. Adv. Manuf. Technol.* **2004**, *23*, 93.
13. Mireles, J.; Adame, A.; Espalin, D.; Medina, F.; Winker, R.; Hoppe, T.; Zinniel, B.; Wicker, R. In Solid Freeform Fabrication (SFF) Symposium, University of Texas: Austin, **2011**; p 185.
14. Williams, C. *Physics World* **2006**, *19*, 24.

15. Reprap Forum, PLA Finishing Experiment, URL: http://forums.reprap.org/read.php?1,281724.
16. La Carrubba, V.; Carfi Pavia, F.; Brucato, V.; Piccarolo, S. *Int. J. Mater. Form.* **2008**, *1*, 619.
17. Young, T. *Philos. Trans. R. Soc.* **1805**, *95*, 65.
18. Owens, D.; Wendt, R. *J. Appl. Polym. Sci.* **1969**, *13*, 1741.
19. Kaelble, D. H. *J. Adhesion* **1970**, *2*, 66.
20. Rabel, W. *Farbe Und Lack.* **1971**, *77*, 997.
21. Ohnesorge, W. *Z. Angew. Math. Mech.* **1936**, *16*, 355.
22. Cappelletti, G.; Ardizzone, S.; Meroni, D.; Soliveri, G.; Ceotto, M.; Biaggi, C.; Benaglia, M.; Raimondi, L. *J. Colloid Interface Sci.* **2013**, *389*, 284.
23. Shin, P.; Sung, J.; Lee, M. H. *Microelectron. Reliab.* **2011**, *51*, 797.